Available online at www.sciencedirect.com
SCIENCE DIRECT
International Journal of Heat and Mass Transfer 49 (2006) 1329–1339
International Journal of HEAT and MASS TRANSFER
www.elsevier.com/locate/ijhmt

Numerical simulation of wall roughness on gaseous flow and heat transfer in a microchannel

Yan Ji, Kun Yuan, J.N. Chung *

Department of Mechanical and Aerospace Engineering, University of Florida, Gainesville, FL 32611-6300, USA

Received 7 March 2005; received in revised form 7 October 2005
Available online 6 December 2005

Abstract

A flow and heat transfer numerical simulation was performed for a 2D compressible gas flow through a microchannel in the slip regime to investigate the effects of wall roughness. The wall roughness is simulated by rectangular microelements. This effect is examined for gas flows under inlet *Mach* number ranging from 0.0055 to 0.202. The numerical results demonstrate that the roughness elements have a significant impact on the flow characteristics. For rarefied gases, it is found that roughness effect leads to an increase in the *Poiseuille* number with increasing roughness height and decreasing element spacing. The surface roughness has a more significant effect on the flow with a lower inlet *Kn*. Compressible gas flow is also sensitive to the height of the wall roughness elements. In addition, an increase of the relative roughness height leads to a pronounced decrease in the local heat flux for both rarefied and compressible flow. The average *Nusselt* numbers have a much more significant reduction for a rarefied flow than a compressible flow. The influence of wall roughness on the average heat transfer rate is smaller than that on the *Poiseuille* number.

Keywords: Roughness effect; Heat transfer; Microchannel; Gaseous flow; Compressibility effect; Rarefaction effect

1. Introduction

Applications of microtechnology must utilize components or systems with microscale fluid flow, and heat and mass transfer. Many reported experiments [1–9] indicate that remarkable differences and conflicts exist in the microchannel flow and heat transfer characteristics compared with those in conventional size channels. For example, Choi et al. [5] found that the *Poiseuille* number, *fRe* (product of the friction factor *f* and Reynolds number *Re*), for laminar nitrogen gas flow in microtubes having diameters smaller than 10 μm was about 53, that is lower than the conventional value of 64. But Wu and Little [1,2] reported that the *Poiseuille* number for very rough microchannel flow was much higher than 64. There may be several main factors responsible for the inconsistency:

(1) *Compressibility effect.* The compressibility is significant when the *Mach* number approaches unity. In a microchannel, the high *Mach* number and large pressure drop can be reached even at low Reynolds numbers. As a result, the variation of gas density and acceleration can occur along the channel, which will lead to an increase in friction factor [10]. Guo et al. [11,12] demonstrated that for a gas flow through a microchannel, the local friction factor was not a constant but increased with increasing local *Mach* number if the inlet *Mach* number was sufficiently high ($Ma > 0.2$). In addition, the local *Nusselt* number increased along the channel due to the compressibility effect.
(2) *Rarefaction effect.* If the *Knudsen* number ($Kn = \lambda/H$, ratio between the gas mean free path and the length scale) is in the range from 0.001 to 0.1, the flow cannot be considered as a continuum flow. Velocity slip and temperature jump occur at the wall surface [13]. Such rarefaction effect leads to a reduction in

* Corresponding author. Tel.: +1 352 392 9607; fax: +1 352 392 1071.
E-mail address: jnchung@ufl.edu (J.N. Chung).

0017-9310/$ - see front matter © 2005 Elsevier Ltd. All rights reserved.
doi:10.1016/j.ijheatmasstransfer.2005.10.011

Nomenclature

c_p	specific heat (J/kg K)
D_h	hydraulic diameter (m)
e	relative roughness height (%)
f	friction factor
H	channel height (m)
K	thermal conductivity (W/m^2 K)
L	channel length (m)
$\vec{n}$	unit inward normal vector from channel walls
P	static pressure (Pa)
r	roughness height (m)
R	gas constant (J/kg K)
s	roughness spacing (m)
T	temperature (K)
u	stream velocity (m/s)
v	normal velocity (m/s)
w	roughness width (m)
C	Poiseuille number
Kn	Knudsen number
Ma	Mach number
Nu	Nusselt number
Pe	Peclet number
Pr	Prandtl number
Re	Reynolds number
U, V	dimensionless velocity
X, Y	dimensionless coordinate variables

Greek symbols

α	thermal diffusion coefficient (m^2/s)
μ	viscosity (m^2/s)
θ	dimensionless temperature
ρ	density (kg/m^3)
σ_T	energy accommodation
σ_v	momentum accommodation
ξ	ratio of channel height to channel length

Subscripts

i	inlet
0	stagnation
w	wall

Superscript

*	dimensionless variable

the friction factor and heat transfer coefficient with increasing Kn number. For air under the standard atmospheric condition, the rarefaction effect becomes important if the hydraulic diameter of a microchannel is less than 67 μm.

(3) *Surface roughness.* At the microscale level, it is impossible to obtain a completely smooth wall surface. According to the traditional knowledge for macrosystems, when the relative roughness is less than 5%, its effect on the friction factor is negligible. But for microscale channels, previously reported experimental and computational results have drawn a conclusion that surface roughness has a significant influence on flow and heat transfer [1,2,14–19]. For example, the experiment by Kandlikar et al. [14] indicated that for a 0.62 mm tube with relative roughness of 0.355%, the effect of roughness on the friction factor and heat transfer was significant. Mala and Li [8] observed that for rough channels with diameters ranging from 50 to 254 μm (relative roughness height 0.7–3.5%), the pressure gradient was higher than that predicted by the classical theory and the friction factor increased when the Re number was increased. In addition, an early transition from laminar to turbulent flow occurred at the Reynolds number less than 2300. They concluded that these phenomena can be well explained due to the surface roughness effects.

However, for a rarefied gas flowing in a microchannel, the roughness effect is more complex and difficult to measure [9,19–26]. Experimental investigation by Sugiyama [19,20] demonstrated that the conductance of an unsteady rarified flow between two flat, rough plates decreased significantly with decrease in Kn when $Kn > 1$. It reached the minimum value around $Kn = 0.5$, and with further decrease in Kn, the conductance increased rapidly. Their calculation also showed that a pronounced effect of the wave angle on the flow conductance, when $Kn = 1$ and $Kn = 0.1$. They did not investigate the roughness effect on rarefied flow in the slip regime ($0.001 < Kn < 0.1$). Similar qualitative results also were obtained by Davis et al. [21]. Recently, Turner et al. [7] experimentally studied the roughness effect on the rarefied flow. Their experiments indicated that when the range of relative surface roughness was $0.1\% < e < 6\%$, there was no clear effect on the friction factor for laminar flows. They pointed out that this result might come from a higher inherent uncertainty of experiment (uncertainty is estimated at 4.7–10.2%). Therefore, it is an experimental problem to exactly estimate to what extent the surface roughness influences the rarefied flow characteristics. In addition, it is difficult to experimentally evaluate the effect of roughness on heat transfer due to small-scale dimensions.

In modeling of roughness effect on rarefied flows, Usami et al. [22] studied rarefied gas flow through a 2D channel using a DSMC method by varying the surface roughness distribution and the Kn number. The reduction of flow conductivity caused by surface roughness was obtained in the transition regime. Sun's study [23] by using a DSMC method found that the roughness element size had a significant effect on the friction factor of rarefied flows when $0.01 < Kn < 0.1$. Karniadakis et al. [24] applied a more

accurate gas flow model and found that the roughness effect becomes more significant on rarefied flows when the *Kn* number was increased. However, to our knowledge, no previous investigations have been reported to study the effect of surface roughness on heat transfer in a rarefied flow. In the present study, a flow and heat transfer model is developed to investigate the roughness effect on rarefied gas flow in microchannels. We will address three following issues: (1) For the gas in slip region ($0.001 < Kn < 0.1$) as the *Knudsen* number increases, whether or not the roughness effect becomes weaker and critically depends on the shape and size of the roughness? (2) For compressible gas, whether or not the roughness effect becomes more significant? (3) To what extent does the effect of different rough elements on the heat transfer?

2. Model development

2.1. Problem statement

We consider a pressure-driven gas flow between two long parallel flat plates. Fig. 1 shows a schematic of the 2D flow through a channel with length L and height H. Elemental microslabs with a rectangular cross section of height r and width w are attached to the inner surfaces of the plates and perpendicular to the flow direction to simulate the wall roughness. These elements are uniformly and symmetrically distributed on the top and bottom surfaces to represent local obstructions similar to those in the study of Hu et al. [16]. Although, this geometry is not exactly the same as the actual rough surface, it is considered as a close approximation to investigate the roughness effect on the flow field and pressure distribution. The distance between the two plates is designated as H, which is also the characteristic length of the flow system. The inlet pressure, density and temperature of the gas flow are P_i, ρ_i, T_i, respectively. The channel surfaces are isothermal and set at T_w which is different from T_i. For the rough elements, the center-to-center spacing between adjacent elements is s. A parameter called "relative roughness height" is defined as $e = r/H$. In most microfluidic systems, the relative roughness heights are estimated at 0.1–6%. We adopt this roughness height range for the study.

Furthermore, other assumptions and limitations inherent to the current model must be pointed out: (1) The flow is limited in the Reynolds number regime of $0.001 < Re < 100$ which is expected in most microfluidic systems. (2) In general, the microchannel characteristic lengths are in the range of 1–100 μm. From the above discussion, we know that the rarefaction effect cannot be neglected. In addition, for the pressure driven gas flow, when the channel length is much larger than the channel height (i.e., $L \gg H$), even in the low Reynolds number range, the *Mach* number can reach a higher value due to small hydraulic diameter and higher pressure drop. The compressibility effect becomes more significant. In the current study, these two effects have been taken into account among different cases.

2.2. Governing equations

As we know, the Navier–Stokes equation is the first order approximation to the Chapman–Enskog solution and can be extended to the slip flow region with the Maxwell's slip boundary condition. A steady laminar flow of compressible fluid with constant thermophysical properties is considered. For the compressible flow, the continuity equation, momentum equations, energy equation and the gas state equation are

$$\frac{\partial(\rho u)}{\partial x} + \frac{\partial(\rho v)}{\partial y} = 0 \tag{1}$$

$$\rho u\frac{\partial u}{\partial x} + \rho v\frac{\partial u}{\partial y} = -\frac{\partial P}{\partial x} + \mu\left[\frac{\partial^2 u}{\partial x^2} + \frac{\partial^2 u}{\partial y^2} + \frac{1}{3}\left(\frac{\partial^2 u}{\partial x^2} + \frac{\partial^2 v}{\partial x\,\partial y}\right)\right] \tag{2}$$

$$\rho u\frac{\partial v}{\partial x} + \rho v\frac{\partial v}{\partial y} = -\frac{\partial P}{\partial y} + \mu\left[\frac{\partial^2 v}{\partial x^2} + \frac{\partial^2 v}{\partial y^2} + \frac{1}{3}\left(\frac{\partial^2 v}{\partial y^2} + \frac{\partial^2 u}{\partial x\,\partial y}\right)\right] \tag{3}$$

$$\begin{aligned}\rho c_p u\frac{\partial T}{\partial x} + \rho c_p v\frac{\partial T}{\partial y} &= \frac{\partial}{\partial x}\left(K\frac{\partial T}{\partial x}\right) + \frac{\partial}{\partial y}\left(K\frac{\partial T}{\partial y}\right) + u\frac{\partial P}{\partial x} + v\frac{\partial P}{\partial y} \\ &\quad + \mu\left[2\left(\frac{\partial u}{\partial x}\right)^2 + 2\left(\frac{\partial v}{\partial y}\right)^2 + \left(\frac{\partial v}{\partial x} + \frac{\partial u}{\partial y}\right)^2\right] - \frac{2}{3}\mu\left(\frac{\partial u}{\partial x} + \frac{\partial v}{\partial y}\right)^2\end{aligned} \tag{4}$$

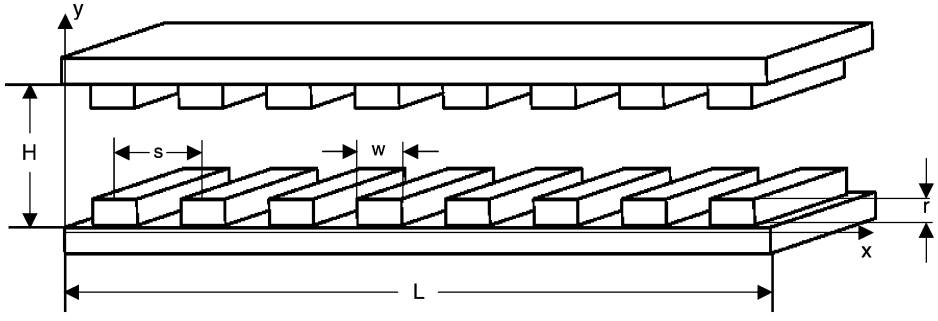

Fig. 1. Schematic and coordinate system of a gas flow through a 2D microchannel with simulated wall roughness elements. (The number of rough elements is not the actual number.)

$$P = \rho RT \tag{5}$$

where T, ρ, P, u and v and are the gas temperature, density, pressure, streamwise velocity, and normal velocity, respectively. c_p, μ and K are the specific heat, viscosity and thermal conductivity of the gas, which are taken as constant. The above equations are non-dimensionalized with respect to the channel height H, inlet mean velocity $\bar{u}_\mathrm{i}$, inlet temperature T_i, inlet mean density $\bar{\rho}_\mathrm{i}$ and inlet pressure P_i. The dimensionless temperature θ, inlet Re_i number, inlet Ma_i, inlet Pe_i number, inlet Kn_i and other variables are defined as

$$\theta = \frac{T - T_\mathrm{w}}{T_\mathrm{i} - T_\mathrm{w}}, \quad Re_\mathrm{i} = \frac{\bar{\rho}_\mathrm{i}\bar{u}_\mathrm{i}H}{\mu}, \quad Ma_\mathrm{i} = \frac{\bar{u}_\mathrm{i}}{\sqrt{\gamma RT_\mathrm{i}}}$$

$$Pe_\mathrm{i} = \frac{\bar{u}_\mathrm{i}H}{\alpha_\mathrm{i}}, \quad Kn_\mathrm{i} = \sqrt{\frac{\pi\gamma}{2}}\frac{Ma_\mathrm{i}}{Re_\mathrm{i}}, \quad \xi = \frac{H}{L}, \quad X = \frac{x}{L}$$

$$Y = \frac{y}{H}, \quad \rho^* = \frac{\rho}{\rho_\mathrm{i}}, \quad P^* = \frac{P}{P_\mathrm{i}}, \quad U = \frac{u}{\bar{u}_\mathrm{i}}$$

$$V = \frac{v}{\bar{u}_\mathrm{i}}, \quad c_p^* = \frac{c_p}{c_{p_\mathrm{i}}}, \quad K^* = \frac{K}{K_\mathrm{i}}$$

Therefore, Eqs. (1)–(4) are non-dimensionalized as

$$\xi\frac{\partial(\rho^* U)}{\partial X} + \frac{\partial(\rho^* V)}{\partial Y} = 0 \tag{6}$$

$$Re_\mathrm{i}\rho^*\left(\xi U\frac{\partial U}{\partial X} + V\frac{\partial U}{\partial Y}\right) = -\frac{\xi Re_\mathrm{i}}{\gamma Ma_\mathrm{i}^2}\frac{\partial P^*}{\partial X} + \left[\xi^2\frac{\partial^2 U}{\partial X^2} + \frac{\partial^2 U}{\partial Y^2} + \frac{1}{3}\left(\xi^2\frac{\partial^2 U}{\partial X^2} + \xi\frac{\partial^2 V}{\partial X\partial Y}\right)\right] \tag{7}$$

$$Re_\mathrm{i}\rho^*\left(\xi U\frac{\partial V}{\partial X} + V\frac{\partial V}{\partial Y}\right) = -\frac{Re_\mathrm{i}}{\gamma Ma_\mathrm{i}^2}\frac{\partial P^*}{\partial Y} + \left[\xi^2\frac{\partial^2 V}{\partial X^2} + \frac{\partial^2 V}{\partial Y^2} + \frac{1}{3}\left(\frac{\partial^2 V}{\partial Y^2} + \xi\frac{\partial^2 U}{\partial X\partial Y}\right)\right] \tag{8}$$

$$\begin{aligned}\xi U\frac{\partial\theta}{\partial X} + V\frac{\partial\theta}{\partial Y} &= \frac{1}{Pe_\mathrm{i}\rho^*}\left[\xi^2\frac{\partial}{\partial X}\left(\frac{\partial\theta}{\partial X}\right) + \frac{\partial}{\partial Y}\left(\frac{\partial\theta}{\partial Y}\right)\right] + Ec_\mathrm{i}\frac{P_\mathrm{i}}{\rho_\mathrm{i}u_\mathrm{i}^2\rho^*}\left[\xi U\frac{\partial P}{\partial X} + V\frac{\partial P}{\partial Y}\right] + \frac{Ec_\mathrm{i}}{Re_\mathrm{i}\rho^*}\left[2\left(\frac{\partial U}{\partial X}\xi\right)^2\right.\\ &\left. + 2\left(\frac{\partial V}{\partial Y}\right)^2 + \left(\frac{\partial V}{\partial X}\xi + \frac{\partial U}{\partial Y}\right)^2 - \frac{2}{3}\left(\xi\frac{\partial U}{\partial X} + \frac{\partial V}{\partial Y}\right)^2\right]\end{aligned} \tag{9}$$

2.3. Boundary conditions

The gas flow is driven by a given pressure difference between the inlet and the outlet of the entire channel length L. The wall temperature is set at a constant temperature T_w, which is higher than the gas flow inlet total temperature T_0. The entire microchannel of length L is taken as the computational domain to investigate the effect of roughness on the flow field and heat transfer. To reduce the computation work, only one half of channel is considered due to the symmetrical conditions that are applied at $Y = 0.5$. So the boundary conditions for this rough channel model are

$$X = 0: \quad P^* = 1, \quad V = 0, \quad \theta = 1 \tag{10}$$

$$X = 1: \quad P^* = P_\mathrm{out}/P_\mathrm{i} \tag{11}$$

On the rough wall:

$$\theta|_\mathrm{w} = \frac{2 - \sigma_T}{\sigma_T}\left(\frac{2\gamma}{\gamma + 1}\right)\frac{1}{Pr}\left[Kn\left(\frac{\partial\theta}{\partial n}\right)_s + \frac{Kn^2}{2}\left(\frac{\partial^2\theta}{\partial n^2}\right)_s\right] \tag{12}$$

$$U|_\mathrm{w} = \frac{2 - \sigma_v}{\sigma_v}\left[Kn\left(\frac{\partial V}{\partial n}\right)_s + \frac{Kn^2}{2}\left(\frac{\partial^2 V}{\partial n^2}\right)_s\right] \tag{13}$$

$$V|_\mathrm{w} = 0 \tag{14}$$

Here, the second order slip conditions suggested by Beskok and Karniadakis [27] are adopted. $U|_\mathrm{w}$ and $V|_\mathrm{w}$ are velocity components which are parallel and normal to wall. $\vec{n}$ is the unit inward normal vector from channel walls. σ_T is energy accommodation coefficient and σ_v is momentum accommodation coefficient. Both σ_T and σ_v vary from 0 to 1.0 depending on the surface roughness, temperature and working medium [28,29]. Here, the two values are set at 0.9 and 0.9, respectively. The inlet stagnation pressure P_0, inlet stagnation temperature T_0 and exit static pressure P_out are given. In fact, the inlet pressure and inlet temperature are determined by the following expressions under isentropic conditions:

$$\frac{p_0}{p_\mathrm{i}} = \left[1 + \frac{(\gamma - 1)}{2}Ma_\mathrm{i}^2\right]^{\gamma/(\gamma-1)} \tag{15}$$

$$\frac{T_0}{T_\mathrm{i}} = \left[1 + \frac{(\gamma - 1)}{2}Ma_\mathrm{i}^2\right] \tag{16}$$

Based on the above boundary conditions, both the flow and heat transfer start to develop from the entrance. In fact, the pressure drop is not linear and therefore the flow cannot reach a fully developed state due to compressible and rarefaction effects in a rough microchannel.

2.4. Additional equations

A parametric study was designed and conducted to investigate the effects of roughness on the gas flow characteristics. The hydraulic diameter D_h, friction factor f, local Re number, *Poiseuille* number C and average Nusselt number, Nu, are defined as the following:

$$D_\mathrm{h} = \frac{4A}{l} = 2H \tag{17}$$

$$fRe = \frac{-2(\mathrm{d}\overline{P}/\mathrm{d}x) \times D_\mathrm{h}^2}{\mu\bar{u}} \tag{18}$$

$$\lambda = \frac{(\overline{fRe})_\mathrm{rough}}{(\overline{fRe})_\mathrm{smooth}} \tag{19}$$

$$Re = \frac{\bar{\rho}_i \bar{u}_i D_h}{\mu} \tag{20}$$

$$C = f \cdot Re \tag{21}$$

$$\overline{Nu} = \frac{Q''_{total} D_h}{\Delta T \cdot k} \tag{22}$$

where Q''_{total} is the total heat flux, and ΔT is the average logarithmic temperature difference.

3. System parameters and numerical solution details

Our simulation is based on six cases as shown in Table 1. As stated above, unlike the liquid flows, the rarefaction and compressibility effects play important roles in gaseous flows and lead to different flow characteristics and heat transfer behavior. These effects are closely related to the microchannel dimensions, inlet *Mach* number, and the roughness elements, etc. We divided the six basic cases into two groups, group RE and group CE. For the two cases in group RE, the rarefaction effect is dominant due to a small inlet *Mach* number. On the other hand, for the four cases in group CE, the compressibility effect is dominant due to high Mach numbers. Nitrogen is chosen as the working gas. The inlet flow total temperature is 300 K. The wall temperature is set at 350 K.

The governing equations with appropriate boundary conditions are solved by employing the SIMPLEC algorithm, a finite volume method [30]. The entire microchannel length is taken as the computational domain to investigate the effect of roughness on the flow field and heat transfer. The grids are refined near the wall region to obtain highly accurate numerical solutions around the roughness elements. The roughness elements have been integrated with the flow region as a part of the computational domain. The interior of roughness elements is considered as a ''virtual flow region'', a gas with an extremely high viscosity. While, on the surface of the rough elements, the slip boundary conditions are implemented. To evaluate the grid size effect on the accuracy of numerical solutions, grid-independence tests were performed as the grid size was refined until acceptable differences between the last two grid sizes were found. For example, we have used the following five grid sizes: 32×16, 64×16, 64×32, 96×32 and 128×40 for Case 1 with $e = 0.75\%$. The maximal difference in fRe between 96×32 and 128×40 grid is 1.73%. By balancing between the computation time and accuracy, the grid size 96×32 was selected.

4. Results and discussion

In this section, the effects of wall roughness are investigated for rarefied gaseous flows (group RE: Cases 1 and 2) and compressible gaseous flows (group CE: Cases 3–6) according to the classification shown in Table 1.

4.1. Flow field

The flow streamline patterns inside the rough microchannel for Case 1 are shown in Fig. 2. It is noticed that the presence of roughness elements obviously perturbs the local flows near the channel wall. For the roughness element with a larger spacing $s = 50\%$H, there is almost no recirculation region between each two elements (Fig. 2(a) and (b)). As the spacing between elements decreases, the recirculation region occurs and grows for larger element heights (Fig. 2(c) and (d)). Further calculations demonstrate that the sizes of recirculation regions for Cases 3–6 are relatively small due to the larger element spacing. Therefore, the formation of recirculation is closely related to the shape of rough elements. Fig. 3 shows the pressure contour and near wall velocity distribution for Case 1. From Fig. 3(b), it can be seen that the slip velocity on the bare wall surface is sharply smaller than that on the surface of a rough element. In addition, it is found that under an equal pressure driving potential, the mass flow rates will be 24.24%, 16.9% and 10.67% less than that of a smooth channel for Case 1 with roughness levels of $e = 6.0\%$, $e = 2.98\%$ and $e = 0.75\%$, respectively, because of the obstruction effect. The gas is compressed in the narrower space and expanded in the wider space, which results in the velocity filed experiencing a periodical expansion–compression cycle. Fig. 3(a) shows that the pressure has sharp drop near entrance ($0 < x < 2.55 \times 10^{-7}$ m). Along the surface of roughness element, the pressure gradient is not monotonically negative ($dP/dx < 0$) like a smooth channel, but has a significant local vibration ($dP/dx < 0$ or $dP/dx > 0$). As a result, this pressure vibration leads to the generation of recirculation zones. As we have expected, the above results indicate that wall roughness exerts a remarkable surface friction effect on the gas flow field. Such an effect will further influence the heat transfer characteristics.

Table 1
Base cases for simulation

Group	Case	Kn_i	Ma_i[a]/Ma_0	L	H	e (%H)	s (%H)	w (%s)	N[b]
RE	1	0.033	~0.006/~0.0066	5	2	0, 0.75, 1.49, 2.98, 6.0	50, 25, 10	67	5, 10 , 25
RE	2	0.0083	~0.0055/~0.006	5	2	0, 0.75, 1.49, 2.98, 6.0	50	67	5
CE	3	0.014	~0.0234/~0.0289	100	4	0, 0.75, 2.98, 6.0	200	67	12
CE	4	0.0103	~0.094/~0.159	100	4	0, 0.75, 2.98, 6.0	200	67	12
CE	5	0.008	~0.152/~0.319	100	4	0, 0.75, 2.98, 6.0	200	67	12
CE	6	0.0044	~0.202/~0.527	100	4	0, 0.75, 2.98, 6.0	200	67	12

[a] The inlet *Ma* numbers are values for smooth channels. For different relative roughness height in each case, the values are different.
[b] N denotes number of roughness element.

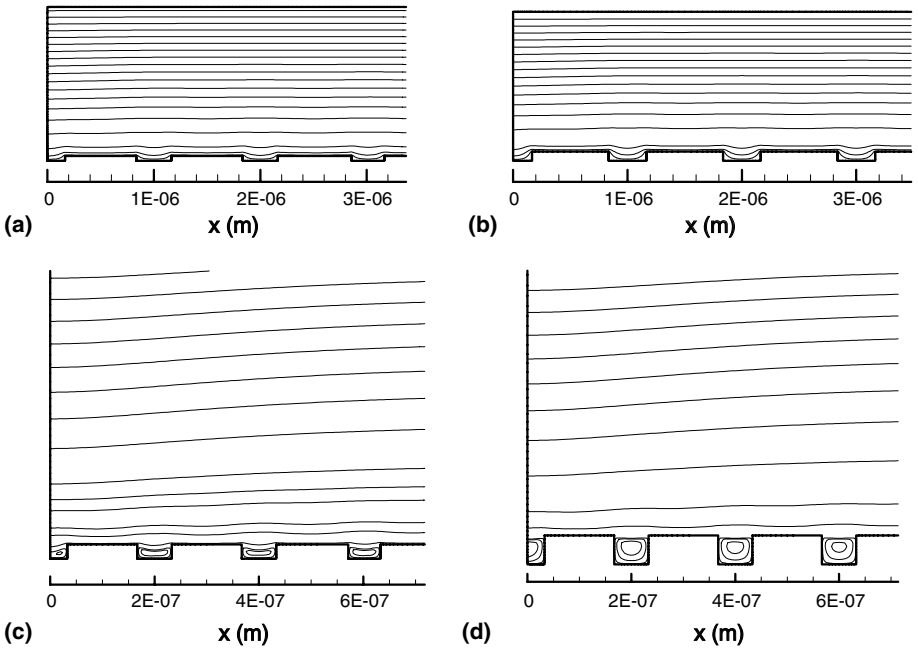

Fig. 2. Streamline contours for Case 1: (a) $e = 2.98\%$, $s = 50\%$H; (b) $e = 6\%$, $s = 50\%$H; (c) $e = 2.98\%$, $s = 10\%$H; (d) $e = 6\%$, $s = 10\%$H.

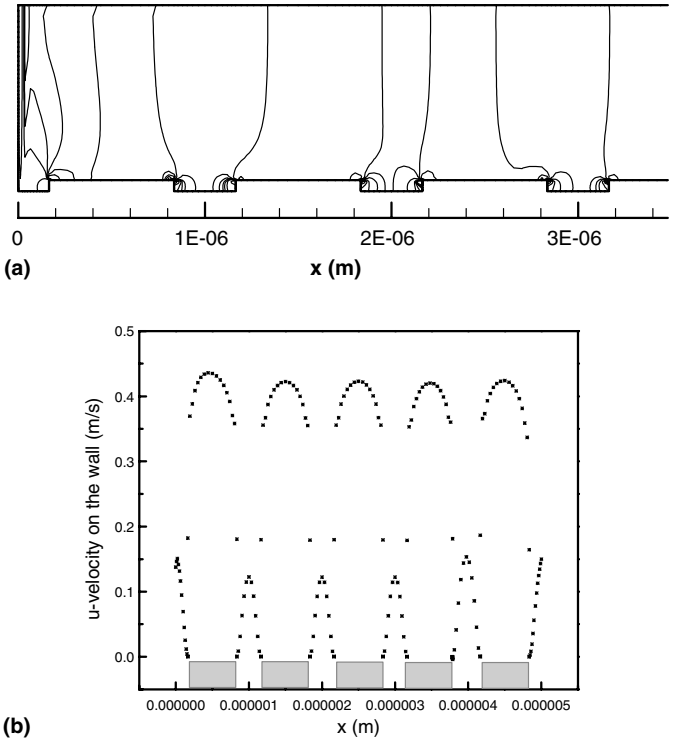

Fig. 3. Pressure contour and near-wall velocity distribution for Case 1 with $e = 6\%$, $s = 50\%$H: (a) pressure contour and (b) u-velocity on the wall.

4.2. Pressure drop and Poiseuille number

4.2.1. Rarefaction effect

In this section, we focus on the effects of roughness in conjunction with rarefaction condition on the gas flow. Cases 1 and 2 are designed to address these two effects together. Fig. 4(a) shows the local friction factor for the smooth channels with different inlet *Kn* numbers. It is clear that *fRe* is significantly lower for the flow with a higher *Kn* than that with a lower *Kn* number. However, near the entrance, the values of *fRe* decrease sharply for both cases. Then, the downstream values of *fRe* decrease slightly along the flow direction. This small change in the *Poiseuille* number along the channel results from an insignificant increase of the *Kn* number. Beskok and Karniadakis [27] recommended a simple equation $fRe = 96/(1 + 6Kn)$ to evaluate the *Poiseuille* number for the rarefied flow with a first order boundary condition and an accommodation coefficient of unity. Comparing results from Beskok and Karniadakis [27] with our results indicates a similar trend except near the entrance region, where our results show an entrance effect. In general, our results are slightly lower. This comes mainly from the lower momentum and energy accommodation coefficients. The lower *Poiseuille* number is expected, since the slip condition implies less shear stress against the wall and a higher *Kn* means larger slip. Therefore, the flow near the entrance is sensitive to the geometry and *fRe* results in high values, while downstream from the entrance, the *fRe* shows smaller decreases.

The average *fRe* for a rough channel is plotted against the relative roughness height in Fig. 4(b). The average *fRe* is evaluated based on the non-entrance region. For the flow with a higher inlet *Kn* number (Case 1), the average *fRe* increase by 11.4%, 14.6%, 18.5%, and 25.8% compared with a smooth channel for relative roughness element heights of 0.75%, 1.49%, 2.98% and 6%, respectively. There is a similar tendency as *Kn* number decreases. However, the surface roughness has a more significant effect on a lower *Kn* flow. For larger relative roughness

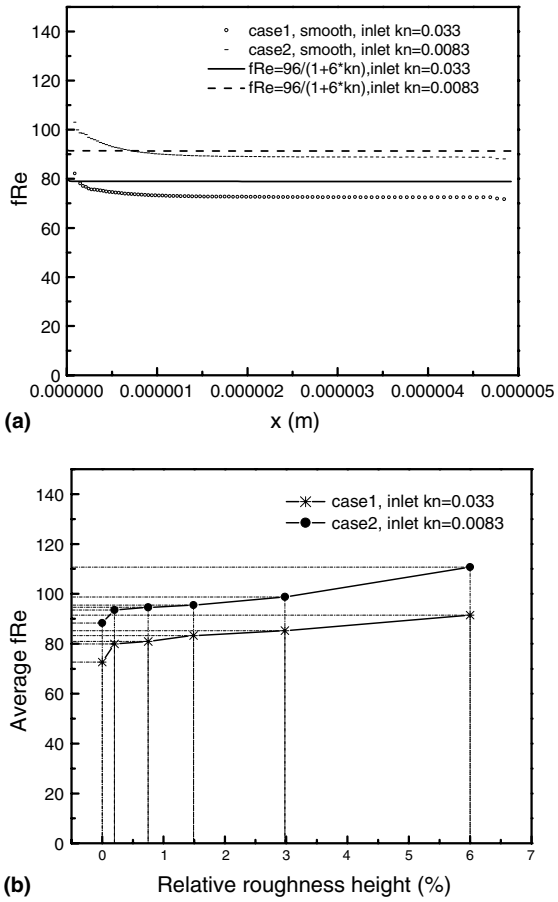

Fig. 4. Effect of *Knudsen* number on a rarefied flow with $s = 50\%$H: (a) *fRe* along the smooth channel and (b) average *fRe* away from the entrance region for a rough channel.

heights ($e \geqslant 2.98\%$), the increase in *fRe* under a lower *Kn* number is more significant than that under a higher *Kn* number. This is because that for lower *Kn* number flows, the collisions between rough walls and gas molecules are more often than those for the higher *Kn* number gas flow. For the gas with a lower *Kn* number, the stagnation region between roughness elements causes a greater pressure drop and a higher increase in *fRe*. Similar results can also be found in the study of Sun [23]. Their calculations indicated that when the *Kn* number increased from 0.02 to 0.08, *fRe* significantly decreased.

4.2.2. Roughness shape effect

As stated above, the roughness elements are an idealized simulation of the actual wall roughness. It is necessary to investigate how the detail dimensions of such geometry influence the rarefied flow characteristics. Fig. 5 shows the effect of different spacing between the roughness elements on the average *fRe* for three different relative roughness heights in Case 1. It is found that the more elements per unit area, the more increase in the average *fRe*. When the element spacing decreases from $0.5H$ to $0.1H$, the *fRe* increases substantially. This is basically due to the increase in the rough element density causing more flow expansion

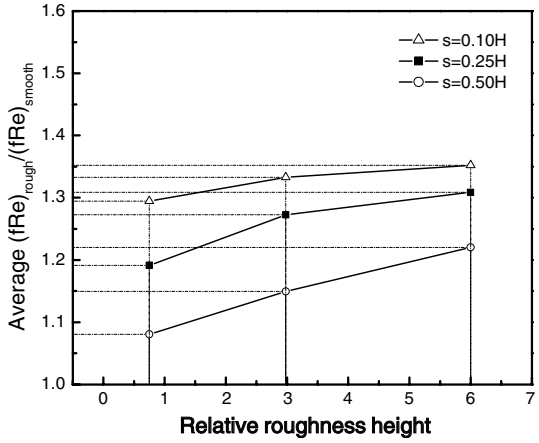

Fig. 5. Effect of roughness on average *fRe* for rarefied flow.

and compression between the roughness elements. Consequently, the pressure drop per unit length increases between the elements and the average *fRe* also increases. In addition, the increase in *fRe* is more pronounced with higher relative roughness heights. However, the roughness spacing, *s*, is only one of the geometric parameters that affect the flow field, other factors such as the shape of element, width and irregularity also have important impacts on the flow field. Croce and Agaro [18] pointed out that the friction factor is very sensitive to the detail structure of the roughness shape. It should be careful to compare the numerical results with the experimental data because there are many higher magnitude uncertainties in experiments at such a small scale level.

4.2.3. Compressibility effect

In this section, we will examine the effect of wall roughness together with the gas compressibility. Cases 3–6 were designed to highlight the compressibility importance. Fig. 6(a) demonstrates that the dependence of the local *fRe* on the local *Ma* number for the compressible flow. The Reynolds number stays constant along the channel but the *Mach* number increases due to the acceleration of the gas flow. After the entrance region, local *fRe* increases along the smooth channel for a compressible flow. For example, when the *Mach* number increases from inlet at 0.202 to outlet at 0.527, *fRe* at outlet reaches to 138. Asako et al. [10] suggested a local *fRe* correlation for a developing compressible flow: $fRe = 96 - 4.55Ma + 274.8 \times Ma^2$. For Case 6, our results of local *fRe* is lower than that obtained from this expression. This is because the rarefaction effect, that is included in the current model but not in Asako et al. [10]. The rarefaction alleviates the friction effect of the wall on the gas flow.

In addition, the increase in average *fRe* for rough channels depends on the inlet *Ma* number as shown in Fig. 6(b). For the incompressible flow, the *Poiseuille* number stays constant with a very large Reynolds number for a given relative roughness height [18]. However, for a compressible flow, the average *fRe* shows significant increases. The

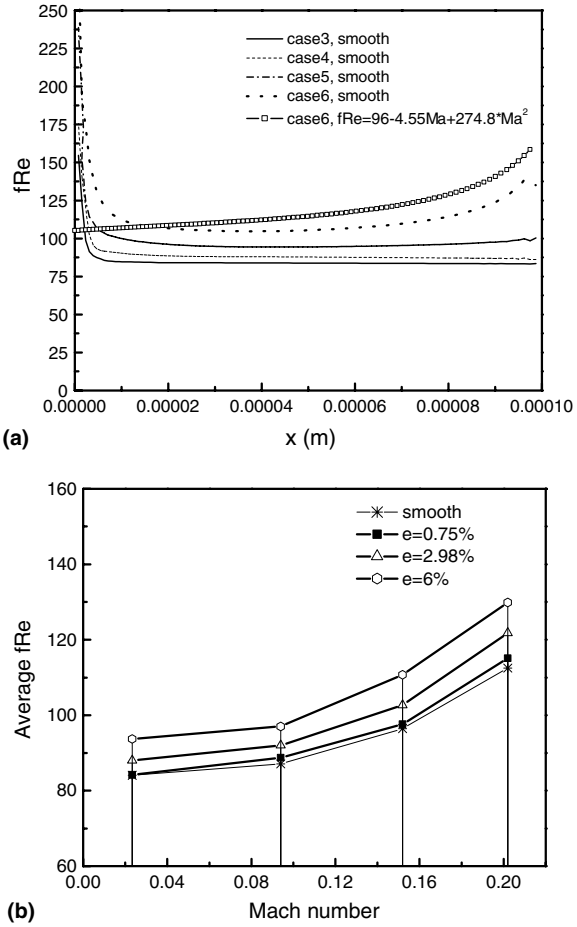

Fig. 6. Effect of wall roughness on *fRe* for compressible flow: (a) *fRe* along the smooth channel and (b) average *fRe* for a rough channel with different *Mach* numbers.

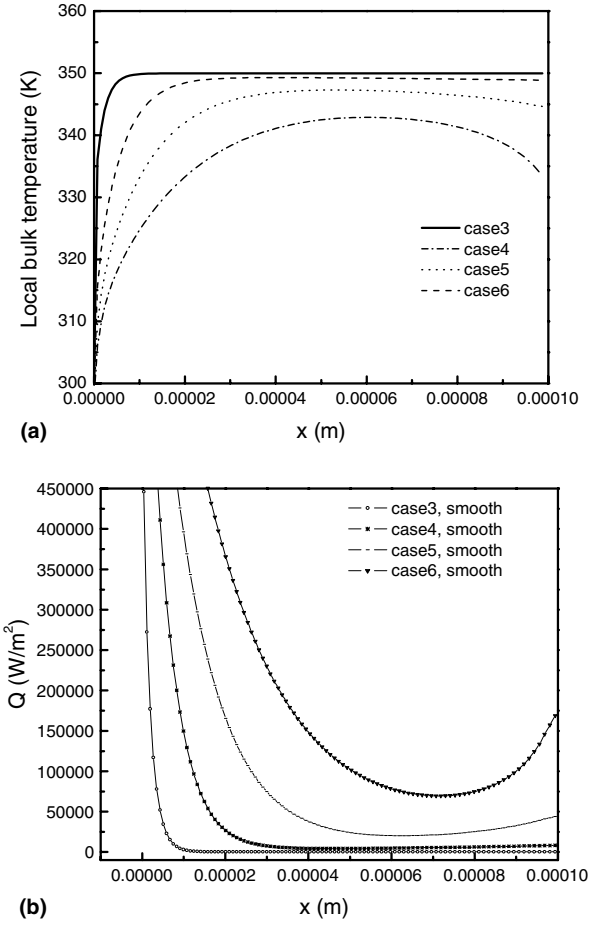

Fig. 7. The local bulk temperature and heat flux for smooth channels: (a) local bulk temperature and (b) local heat flux.

increase in the average *fRe* is most significant in a rough channel with a larger *Ma* number and the highest roughness element. This is because the *Mach* number represents the magnitude of compressibility of a gas flow. The higher the *Mach* number is, the more the velocity profile deviates from the parabolic shape and the larger the *Poiseuille* number becomes. Therefore, the compressible gas is still sensitive to the rough surface. However, the experimental result by Turner et al. [7] demonstrated that when the range of relative surface roughness was $0.1\% < e < 6\%$, there was no clear effect on the friction factor for rarefied and compressible flows. The increase in *fRe* appeared to be quite small and is within 2–6%. They pointed out that this result might come from no statistical difference between smooth and rough channels and a higher inherent uncertainty of experiment. The present model is based on a 2D and idealized rough elements, so the effect of roughness on flow could be slightly overestimated.

4.3. Heat transfer

In this section, the effect of wall roughness on the heat transfer is investigated. To provide a basis for comparison, the local flow bulk temperatures and heat fluxes from the wall of smooth channels for Cases 3–6 are plotted in Fig. 7(a) and (b). For the flow at a low inlet *Mach* number (Case 3), the bulk temperature rises very quickly and then asymptotically approaches the wall temperature of 350 K. Accordingly, the heat flux sharply decreases from a large value at the inlet to a diminishingly small quantity in a relatively short distance. For the gas flow with a higher inlet *Mach* number, the bulk temperature falls near the exit because much thermal energy converses into the kinetic energy. Accordingly, the local heat fluxes at the wall do not decrease monotonously along the channel, but increase near the outlet.

The effect of wall roughness on the heat transfer for a rarefied flow is shown in Fig. 8(a) and (b). For the gas flow with a larger inlet *Kn* number, the rarefaction effect is stronger and the local heat flux is much lower than that with a smaller *Kn* number in the region close to the entrance as shown in Fig. 8(a). The gas temperature on the wall is lower. This mainly results from the fact that the thermal transport by collision between the gas molecules and the wall is less often and hence less energy is transferred to the gas flow. As seen from Fig. 8(b), an increase of the relative roughness height leads to a pro-

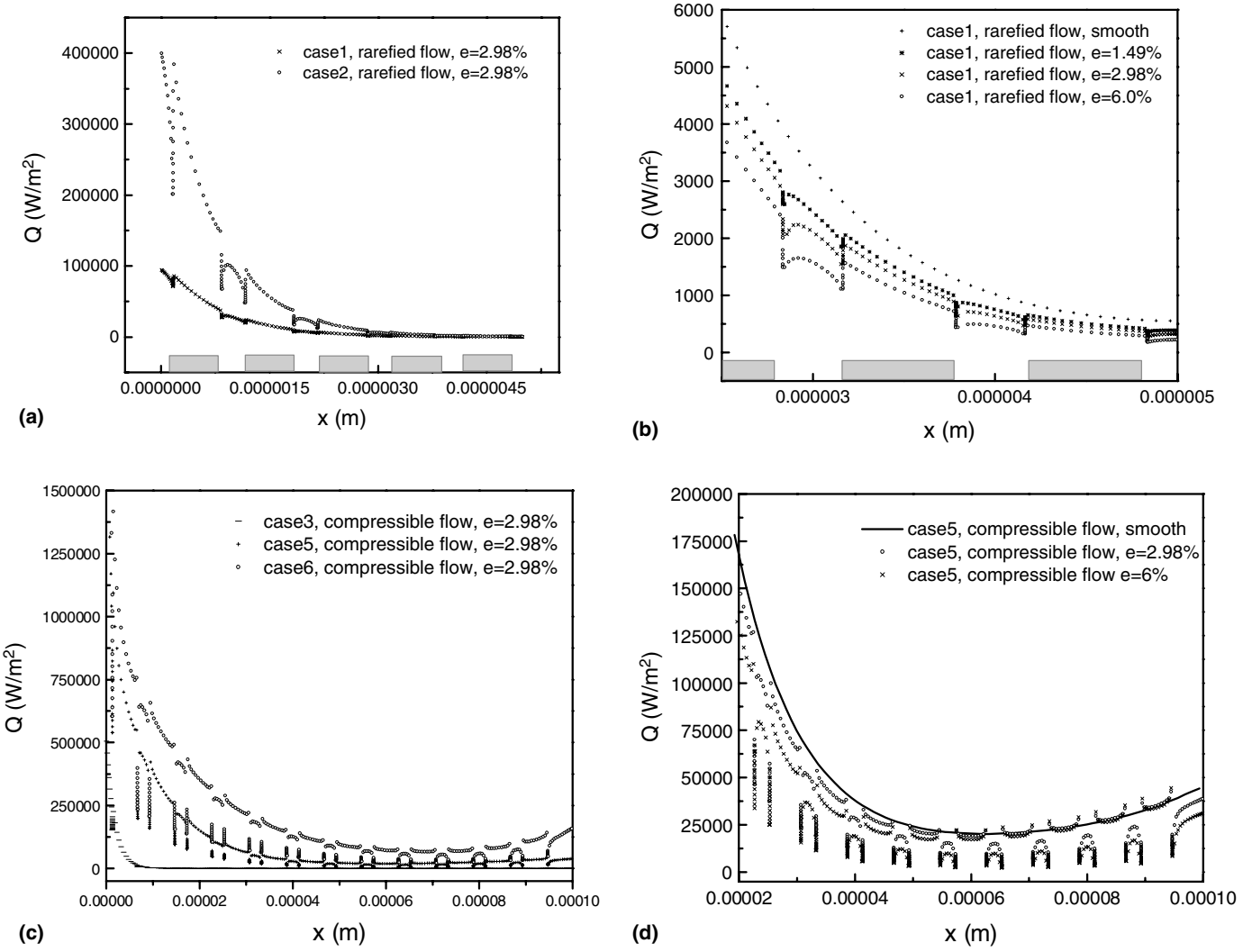

Fig. 8. Effect of wall roughness on the heat transfer: (a) for rarefied flows with different inlet *Kn* numbers, (b) for rarefied flows with different *e*'s, (c) for compressible flows with different inlet *Ma* numbers, (d) for compressible flows with different *e*'s.

nounced decrease of the local heat flux on the bare wall surface portion. The reduction in bulk velocity and increase in the height of recirculation region make the flow field well mixed locally and thus cause the temperature gradient near the wall to decrease. Therefore, the heat transfer rate at this region is lower, especially at the region near the element corner. However, on the surfaces of the roughness elements, the local heat transfer rate is higher due to a higher velocity. With an increase of the inlet *Mach* number, the compressibility effect becomes more prevalent and the rarefaction effect is relatively weaker. Local heat flux on the wall increases as the inlet *Mach* number is increased for a given relative roughness height as shown in Fig. 8(c). For the gas flow with a weak compressibility (Case 3), there is almost no difference in the local heat flux between at the "valley" and at the "peak" of roughness elements. While for the gas flow with a high compressibility (Case 6), this difference becomes significant. By comparing Fig. 8(d) with Fig. 8(b), it can be seen that the reduction in the local heat flux on the bare wall surface portion for a high compressible flow is much more pronounced than a rarefied flow.

Fig. 9 shows that the effect of wall roughness on the average *Nu* number. The average *Nu* numbers decrease for rarefied flows in rough channels. Especially, for the rarefied flow with higher *Kn* numbers, the reduction in *Nu* number with an increase of the roughness height is much more significant, which means that the efficiency of heat transfer decreases. However, for a highly compressible flow (Cases 5 and 6), the average *Nu* numbers do not decrease much or increase slightly with the increase in the roughness height. For Case 3, the rarefaction effect is strong and the compressibility is weaker, the average *Nu* number still is lowered. Therefore, the presence of wall roughness improves the heat transfer for a highly compressible flow. It should be pointed out that the variation of an average *Nu* number is less sensitive to the roughness height as compared to the average *fRe* for a compressible flow. For example, the variation of the *Poiseuille* number in Case 5 with $e = 6.0\%$ can be as high as 14.12% over the smooth

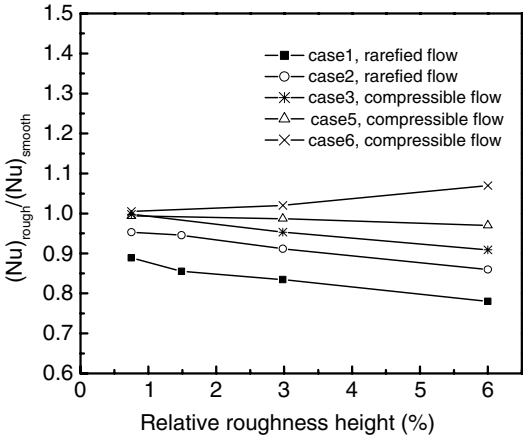

Fig. 9. Effect of wall roughness on the average Nusselt number.

channel, while the average *Nu* number variation is only about 3% lower than the smooth channel.

5. Summary and conclusion

The effects of wall roughness on the rarefied and compressible gas flows were evaluated and the following conclusions were reached:

(1) The rough elements restrict the upstream gas flow and cause more pressure drop and increases *in the Poiseuille* number due to the obstruction effect and formation of recirculation regions. The effect of surface roughness is less pronounced for the rarefied gas.
(2) Rarefied flow is sensitive to the shape of roughness elements. The average *Poiseuille* number increases not only as the roughness height is increased but also as the spacing distance between the roughness elements is decreased. However, this effect is much stronger on the gas flow with a lower *Kn*. Compressible gas flow is still sensitive to the height of the roughness elements.
(3) An increase of the relative roughness height leads to a pronounced decrease in the local heat flux for both rarefied and compressible flows. For rarefied flows, the roughness elements do not improve the average *Nu* number, i.e., the efficiency of heat transfer. When the inlet *Kn* number is larger, the local heat flux and average *Nu* number are greatly lower than those with a smaller *Kn* number. However, for a highly compressible flow, the average *Nu* number does not change much or increases slightly. The existence of wall roughness enhances the heat transfer. The influence of wall roughness on the average heat transfer is smaller than that on the *Poiseuille* number.

Although this theoretical model is proposed based on a simplified 2D uniformly distributed roughness element geometry, which is not the same as the actual rough surface in experiments and it could overestimate the roughness effect, but it provides some insights and qualitative assessment on the effects of wall roughness on the gas flow. The above results indicate that the wall roughness potentially causes more impacts on the flow in the case of microchannels than in conventional channels. However, we should be very careful in explaining the discrepancies between experimental data obtained from microscale and macroscale channels because the surface effect is always coupled with other competing effects, such as compressibility and rarefaction effects.

Acknowledgements

This research was partially supported by Andrew H. Hines, Jr./Florida Progress Endowment Fund. Support from the Department of Mechanical and Aerospace Engineering at the University of Florida is also appreciated.

References

[1] P.Y. Wu, W.A. Little, Measurement of friction factor for the flow of gases in very fine channels used for microminiature Joule–Thomson refrigerator, Cryogenics 23 (1983) 273–277.
[2] P.Y. Wu, W.A. Little, Measurement of the heat transfer characteristics of gas flow in fine channel heat exchangers used for microminiature refrigerators, Cryogenics 24 (1984) 415–420.
[3] J. Pfahler, H. Harley, H. Bau, J.N. Zemel, Gas and liquid flow in small channels, ASME DSC-32 (1991) 49–60.
[4] B.X. Wang, X.F. Peng, Experimental investigation of liquid forced-convection heat transfer through microchannels, Int. J. Heat Mass Transfer 37 (1994) 73–82.
[5] S.B. Choi, R.F. Barron, R.O. Warrington, Fluid flow and heat transfer in micro tubes, ASME DSC-32 (1991) 123–134.
[6] S.S. Hsieh, H.H. Tsai, C.Y. Lin, C.F. Huang, C.M. Chien, Gas flow in a long microchannel, Int. J. Heat Mass Transfer 47 (2004) 3877–3887.
[7] S.E. Turner, Experimental investigation of gas flow in microchannels, ASME J. Heat Transfer 126 (2004) 753–762.
[8] G.M. Mala, D. Li, Flow characteristics of water in microtubes, Int. J. Heat Mass Transfer 20 (1999) 142–148.
[9] S.E. Turner, H. Sun, M. Faghri, O.J. Gregory, Effect of surface roughness on gaseous flow through micro channels, 2000 IMECE, HTD 366 (2) (2000) 291–298.
[10] Y. Asako, T. Pi, S.E. Turner, M. Faghri, Effect of compressibility on gaseous flows in micro-channels, Int. J. Heat Mass Transfer 46 (2002) 3041–3050.
[11] Z.Y. Guo, X.B. Wu, Compressibility effect on the gas flow and heat transfer in a microtube, Int. J. Heat Mass Transfer 46 (1996) 3251–3253.
[12] Z.Y. Guo, X.B. Wu, Further study on compressibility effects on the gas flow and heat transfer in microtube, Microscale Thermophys. Eng. 2 (1998) 111–120.
[13] E.B. Arkilic, M.A. Schmidt, K.S. Breuer, Gas. Slip Flow Long Microchan. 6 (1997) 167–178.
[14] S.G. Kandlikar, S. Joshi, S. Tian, Effect of channel roughness on heat transfer and fluid flow characteristics at low Reynolds numbers in small diameter tubes, in: Proceedings of NHTC'01 35th National Heat Transfer Conference, Anaheim, CA, June 2001, pp. 1–10.
[15] W. Qu, G.M. Mala, D. Li, Heat transfer for water flow in trapezoidal silicon microchannel, Int. J. Heat Mass Transfer 43 (2000) 3925–3936.
[16] Y. Hu, C. Werner, D. Li, Influence of three-dimensional roughness on pressure-driven flow through microchannels, ASME J. Fluid Eng. 125 (2003) 871–879.

[17] Z.Y. Guo, Z.X. Li, Size effect on microscale single-phase flow and heat transfer, Int. J. Heat Mass Transfer 46 (2003) 149–159.
[18] G. Croce, P.D. Agaro, Numerical analysis of roughness effect on microtube heat transfer, Superlatt. Microstruct. 35 (2004) 601–616.
[19] W. Sugiyama, T. Sawada, K. Nakamori, Rarefied gas flow between two flat plates with two dimensional surface roughness, Vacuum 47 (1996) 791–794.
[20] W. Sugiyama, T. Sawada, M. Yabuki, Y. Chiba, Effects of surface roughness on gas flow conductance in channels estimated by conical roughness model, Appl. Surf. Sci. 169–170 (2001) 787–791.
[21] D.H. Davis, L.L. Levenson, N. Milleron, Effects of ''rougher-than-rough'' surfaces on molecular flow through short ducts, J. Appl. Phys. 35 (1964) 529–532.
[22] M. Usami, T. Fujimoto, S. Kato, Mass-flow reduction of rarefied flow roughness of a slit surface, Trans. Jpn. Soc. Mech. Eng., B 54 (1988) 1042–1050.
[23] H. Sun, M. Faghri, Effect of surface roughness on nitrogen flow in a microchannel using the direct simulation Monte Carlo method, Numer. Heat Transfer Part A 43 (2003) 1–8.
[24] G.E. Karniadakis, A. Beskok, Micro Flows, Fundamental and Simulation, Springer, Berlin, 2002.
[25] W.L. Li, J.W. Lin, S.C. Lee, M.D. Chen, Effects of roughness on rarefied gas flow in long microtubes, J. Micromech. Microeng. 12 (2002) 149–156.
[26] T. Veijola, Model flow resistance of a rare gas accounting for surface roughness, in: Proceedings of Nanotech 2003, San Francisco, vol. 2, 2003, pp. 492–495.
[27] A. Beskok, G.E. Karniadakis, A model for flows in channels, pipes and ducts at micro and nanoscales, Microscale Thermophys. Eng. 3 (1999) 43–77.
[28] J.H. Park, S.W. Baek, Investigation of influence of thermal accommodation on oscillating micro-flow, Int. J. Heat Mass Transfer 47 (2004) 1313–1323.
[29] E. Arkilic, K.S. Breuer, M.A. Schmidt, Mass flow and tangential momentum accommodation in silicon micromachined channels, J. Fluid Mech. 437 (2001) 29–43.
[30] S.V. Patankar, Numerical Heat Transfer and Fluid Flow, Hemisphere, Washington, DC, 1980.